

GEOMETRIC ACCURACY OF IKONOS GEO PANCHROMATIC ORTHOIMAGE PRODUCTS

M. A. Aguilar ^{a*}, F.J. Aguilar ^a, F. Carvajal ^a, F. Agüera ^a, L. Estrada ^b

^a Departamento de Ingeniería Rural, EPS, Universidad de Almería, 04120 - La Cañada de San Urbano, Almería, Spain- (maguilar, faguera, faguilar, carvajal)@ual.es

^b Instituto Tecnológico Superior de Tierra Blanca, Prol. Av. Veracruz s/n. Esq. Héroes de Puebla y Corregidora, Col. PEMEX, C.P. 95180, Tierra Blanca, Veracruz, México – luciana1783mx@yahoo.com.mx

Commission I, WG I/5

KEY WORDS: Photogrammetry, IKONOS, Very high resolution, Accuracy, Orthorectification, Geometric modelling

ABSTRACT:

The new very high space resolution satellite images, such as QuickBird and IKONOS, open new possibilities in cartographic applications. This work has as its main aim the assessment of different sensor models for achieving the best geometric accuracy in orthorectified imagery products obtained from IKONOS Geo Ortho Kit Imagery. Two dimensional Root Mean Square Error (RMSE_{2D}) is computed and utilized as accuracy indicator. The ancillary data were generated by high accuracy methods: (1) Check (ICPs) and control points (GCPs) were measured with a differential global positioning system (DGPS) and, (2) a digital elevation model (DEM) with grid spacing of 5 m derived from digitized contour lines with an interval of 10 m and extracted from the 1:10,000 Andalusia Topographic Maps series (RMSE_Z<1.75 m), was used for image orthorectification process. Four sensor models were used to correct the satellite data: (1) First order 3D rational functions without vendor image support data (RFM1), (2) 3D rational functions refined by the user with zero order polynomial adjustment (RPC0), (3) 3D rational functions refined by the user with first order polynomial adjustment (RPC1), and (4) the 3D Toutin physical model (CCRS). The number of control points per orthorectified imagery (9 and 18 GCPs) and their distribution (random and stratified random sampling) were studied as well. The best results, both in the phase of sensor orientation (RMSE_O about 0.59 m) as in the final orthoimages (RMSE_{ORTHO} about 1.25 m), were obtained when the model RPC0 was used. Neither a large number of GCPs (more than nine) nor a better distribution (stratified random sampling) improved the results obtained from RPC0.

1. INTRODUCTION

With the successful launch of very high resolution (VHR) satellites, especially IKONOS in September of 1999, with 1 m Ground Sample Distance (GSD), and QuickBird in October of 2001, with 0.61 m GSD, many researchers have considered them as possible substitutes of the classical aerial images used for cartographic purposes at large scales (Fraser, 2002; Kay *et al.*, 2003; Chmiel *et al.*, 2004; Pecci *et al.*, 2004).

To update an existing cartography or to generate a new cartography from VHR satellite imagery, the raw images must be corrected geometrically to obtain orthorectified images using a digital elevation model (DEM). The necessary steps in this process are: (1) acquisition of image(s) and metadata, (2) acquisition of the coordinates X , Y , Z of ground control points (GCPs) and independent check points (ICPs), (3) obtaining the image coordinates of these points, (4) computation of the unknown parameters of the 3D geometric correction model used, and (5) image(s) orthorectification using a DEM.

The geometric accuracy in orthorectified imagery obtained from panchromatic raw imagery of VHR sensors depends on the quality of the ancillary data (GCPs, DEM), number and distribution of the GCPs in the scene (Zhou and Li, 2000), image pointing of GCPs and, of course, the sensor model used to correct the satellite imagery.

This paper is focused on geometric accuracy issues of Geo Ortho Kit panchromatic image orthorectification. Thus, the influence of factors such as the number and distribution of

GCPs and the sensor model used for the geometric corrections of the satellite image have on the geometric accuracy obtained in the phase of sensor orientation and in the final orthoimage have been evaluated.

2. STUDY SITE AND DATA SET

2.1 Study site

The study site is located at the north-east of Almería City, Spain, specifically in the region of Campo de Níjar.

It is a zone occupied principally by greenhouses, presenting a quiet flat relief, though there is a mountain range that crosses the scene along direction south-west. Figure 1 shows the DEM corresponding to the study area on the European Datum ED50 with the Hayford International Ellipsoid and projection UTM 30 N. The area has an elevation range of between 45 m to 361 m above sea level.

2.2 IKONOS Geo Ortho Kit panchromatic image

In September 2005, we acquire from European Space Imaging® an archive image of IKONOS Geo Ortho Kit. It was taken on 2 June 2005. The image was occupying approximately 11 km per 13 km and was centred on the coordinates, easting and northing respectively, 574,639 m and 4,083,543 m. Other characteristics of the IKONOS image are shown in table 1.

* Corresponding author.

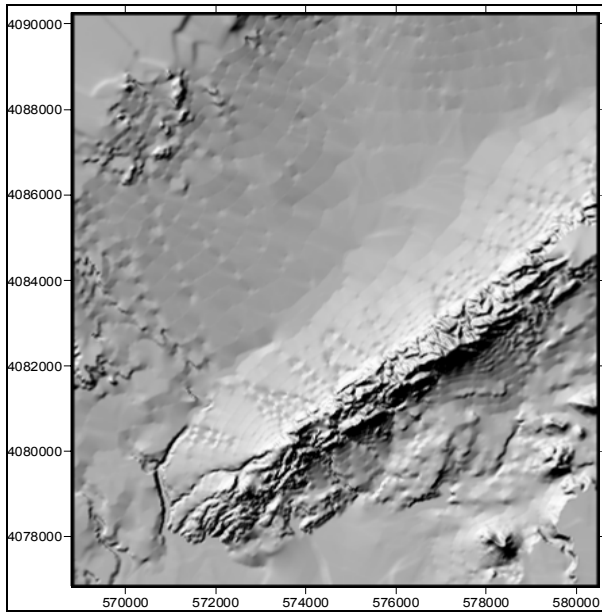


Figure 1. Digital elevation model of the study area.

Product	IKONOS Geo Ortho Kit
Acquisition Date	02/06/05
Cloud Cover (%)	0
Source Image ID	2005060211045020000011316301
Scene ID	2000000978101R10
Sun Angle Azimuth	132.6703 degrees
Sun Angle Elevation	70.22313 degrees
Elevation Angle	78.41 degrees
Collection Azimuth	134.85 degrees
Acquired Nominal GSD	0.84 m
Product Pixel Size	1 m

Table 1. Characteristics of the IKONOS Geo Ortho Kit Image acquired at the study site.

IKONOS Geo Ortho Kit is the IKONOS's commercial imagery format that presents the least level of corrections, both radiometric and geometric. Geo Ortho Kit images include the camera geometry obtained at the time of the image collection. With the Geo Ortho Kit, users can produce their own highly accurate orthorectified products by utilizing commercial off the shelf software, DEMs, and GCPs.

2.3 Ground Control Points

The measurement of GCPs and ICPs was done using Differential Global Positioning System (DGPS) receivers in both static and real-time kinematic (RTK) modes, with post-processing in both cases (Aguilar *et al.*, 2005a). The goal was to obtain a reliable measurement of ground points with accuracy better than a 0.10 m. As a final result of the methodology described the UTM ED 50 coordinates were obtained as well as the orthometric levels in 109 ground points. The selection of the GCPs and ICPs used in this study was based on well-defined and homogeneously distributed points over the IKONOS image (Fig. 2).

2.4 Digital Elevation Model

For the generation of panchromatic orthoimages from IKONOS Geo Ortho Kit, a DEM with a grid spacing of 5 m was used.

The DEM was derived by ourselves from digitized contour lines 10 m interval, extracted from the 1:10,000 Andalusia Topographic Maps series. The vector file was imported to OrthoEngine, from PCI Geomatica, and finite difference algorithms were used to interpolate the grid DEM.

The statistics of the differences of 50 known DGPS coordinates, placed on the natural terrain, minus the DEM were: mean error = -0.53 m, vertical root mean square error ($RMSE_z$) = 1.75 m, maximum error = 4.38 m. These statistics were obtained using SURFER v. 8 (Golden Software), and the DEM extracted from OrthoEngine was also interpolated using radial basis functions (Aguilar *et al.*, 2005b).

2.5 Sensor models used

In satellite imagery, a sensor model or geometric correction model relates object point positions (X, Y, Z) to their corresponding 2D image positions (x, y). In aerial photogrammetry it is solved by means of the known co-linearity equation (e.g. Wong, 1980).

Several sensor models can be used to correct satellite imagery: 2D polynomial functions, 3D polynomial functions, affine model, 3D rational functions and 3D physical models (Tao and Hu, 2001; Jacobsen, 2002; Fraser *et al.*, 2002; Fraser and Yamakawa, 2004; Toutin, 2004). PCI Geomatica OrthoEngine software v. 9.1.7, developed by PCI Geomatics was used for the four sensor models tested in this work.

1.- First order 3D rational functions without vendor image support data (RFM1).

The general form of 3D rational functions is:

$$x = \frac{P_1(X, Y, Z)}{P_2(X, Y, Z)}; y = \frac{P_3(X, Y, Z)}{P_4(X, Y, Z)} \quad (1)$$

Where x and y are the row and column in the image respectively, X, Y and Z are the coordinates of points in object space, and, P_i ($i=1, 2, 3,$ and 4) are polynomial functions with the following general form for the first order solution:

$$P_i = a_{1i} + a_{2i} \cdot X + a_{3i} \cdot Y + a_{4i} \cdot Z \quad (2)$$

Bearing in mind that the first coefficient in the denominator is usually known ($a_{12}=a_{14}=1$) a minimum of 7 GCPs are required to resolve the first order rational polynomial function (RFM1).

2.- Third order 3D rational functions with vendor's rational polynomial coefficients (RPCs) data and refined by a zero order polynomial adjustment (RPC0).

The primary limitation of the approach based exclusively in the vendor distributed RPCs (without GCPs) seems to be the inherent positional biases that arise from systematic errors. These biases can be removed by means of indirect methods if at least one GCP is known.

OrthoEngine's RPC indirect method is based on the block adjustment method published by Grolecki and Dial (2003) for image space (equation 3), where a_0, a_1, a_2, b_0, b_1 and b_2 are the adjustment parameters of an image, Δx and Δy express the discrepancies between the measured line and sample coordinates for the news GCPs in the image space (x', y') and the RPCs projected coordinates for the same GCPs (x, y).

$$\Delta x = x' - x = a_0 + a_1 \cdot x + a_2 \cdot y \quad (3)$$

$$\Delta y = y' - y = b_0 + b_1 \cdot x + b_2 \cdot y$$

For the zero order transformation, only a simple shift (a_0 and b_0) are computed. Because of it, only one GCP is necessary to calculate this indirect method. For IKONOS images, the zero order polynomial adjustment is adequate for most cases, while for QuickBird images a first order polynomial adjustment is required to achieve the best results (Cheng *et al.*, 2005).

3.- Third order 3D rational functions with vendor's RPCs data and refined by a first order polynomial adjustment (RPC1). In this case 6 coefficients of the equation 3 have to be computed (a_0, a_1, a_2, b_0, b_1 and b_2). Therefore it is necessary to know at least three GCPs.

4.- A 3D physical model developed by Dr. Toutin at the Canada Centre for Remote Sensing (Toutin and Cheng, 2002; Toutin, 2003) is also tested in this work (CCRS) for the IKONOS imagery. This physical model was initially developed for medium-resolution sensors in the visible and infra-red as well as in the microwave (Toutin, 1995). Even though the detailed sensor information for IKONOS has not been released by Space Imaging, a valid solution for CCRS can be obtained using a limited number of GCPs (4-6) and basic information from the image metafiles (Toutin and Cheng, 2000).

3. METHODOLOGY

In order to obtain the aims of the work, two tests were carried out.

3.1 Sensor Orientation Error

The aim of this test is to observe the two dimensional root mean square error ($RMSE_{2D}$) in the sensor orientation phase, depending on, first, the number and distribution of the GCPs which take part in the model adjustment, and second, the sensor model used. In this way, 15 repetitions of 9 and 18 GCPs respectively were extracted from 109 initial GCPs. The samplings were carried out in two different ways: (1) completely random sampling, and (2) stratified random sampling, choosing one or two GCPs in each of the sub-areas in which IKONOS scene was divided (Fig. 2). Therefore a total of 60 GCPs combinations were extracted. It seems to be clear that the distribution of 30 combinations of 9 and 18 GCPs carried out according to a completely random sampling should be worse than those carried out by means of a stratified random sampling, due to the fact that in the first case, we can not ensure that at least one GCP per sub-area of IKONOS scene is present in every extracted combinations.

The $RMSE_{2D}$ (equation 4) in the rest of ground points (100 or 91 ICPs respectively) was computed for every combination of GCPs. The variability of the $RMSE_{2D}$ around its mean value estimated from 15 repetitions over the both types of samplings and the number of GCPs was represented as error bars at the 95% confidence interval.

$$RMSE_{2D} = \sqrt{RMSE_x^2 + RMSE_y^2} \quad (4)$$

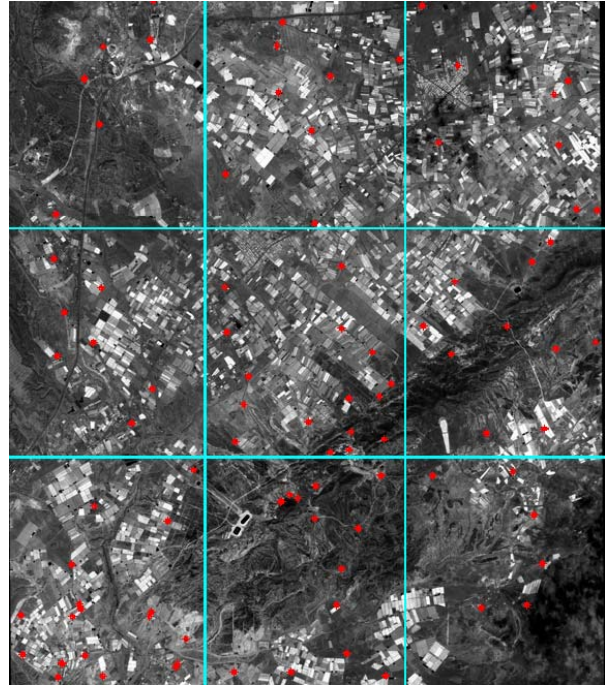


Figure 2. Distribution of 109 ground points (GCPs and ICPs) overlaid on the IKONOS Geo Ortho Kit panchromatic image.

3.2 Orthorectified Image Error

With this second test we will know the geometric accuracy that finally we will have in the orthorectified image, using the previously described DEM. This accuracy ($RMSE_{2D}$) has been calculated over 100 ICPs (Fig. 7) well-defined and homogeneously distributed on the IKONOS scene. ICPs ground coordinates have been extracted from a vectorial cartography at scale 1:1,000 generated in 2002 by our research group (AGR-199) by order of the Council of Agriculture of Andalusia Government. Most of these points are corners of greenhouses that can be pointed very well on IKONOS image.

Only eight orthoimages were pointed. Four of them were obtained from one combination of 18 GCPs chosen with a stratified random sampling, and the four remaining ones, from one combination of 9 GCPs also chosen by means of a stratified random sampling.

The digital orthophotos created have a GSD of 1 m. In the process of orthorectification, the radiometric operation uses a resampling kernel applied to original image cells. The best results are obtained with the sinusoidal resampling kernel ($\sin(x)/x$ with 16×16 windows) (Toutin, 2004). This one was the resampling method used in the eight orthorectified images generated in this work.

4. RESULTS AND DISCUSSION

4.1 Sensor Orientation Error

The figure 3 shows the mean values and confidence intervals at 95% of the $RMSE_{2D}$ obtained for all 15 combinations of 9 GCPs chosen by random sampling. The sensor models RFM1 and CCRS, for this order, show the worse results, with mean values of $RMSE_{2D}$ of 2.67 m and 2.09 m respectively. Besides, it is necessary to emphasize the high standard deviation generated in all 15 repetitions obtained with these two sensor models, which provokes high confidence intervals. It is known the great sensibility that the RFM presents both to the number of GCPs (Davis and Wang (2003) demonstrated that the RFM

model tended to require about 0.4 GCPs km⁻² with IKONOS imagery) and to its distribution (Toutin, 2004; Tao and Hu, 2001). Slightly more strange seems to be the high confidence interval that presents the CCRS model. According to bibliography this sensor model should present a great robustness over the full image using only a few GCPs (Toutin and Cheng, 2000; Cheng *et al.*, 2003). Nevertheless, it is difficult to develop a parametric sensor model which reflects the physical reality of the complete viewing geometry for IKONOS sensor with an absence of detailed sensor information (Tao *et al.*, 2004). For the models using the RPCs given by vendor, the mean values of RMSE_{2D} are around 0.60 m for RPC0 and 0.82 m for RPC1.

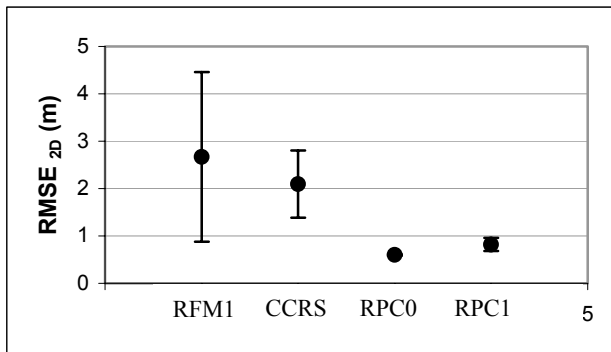


Figure 3. RMSE_{2D} over 100 ICPs with the sensor models used for 9 GCPs random sampling. The black circles represent the mean values and the error bars show the 95% confidence interval.

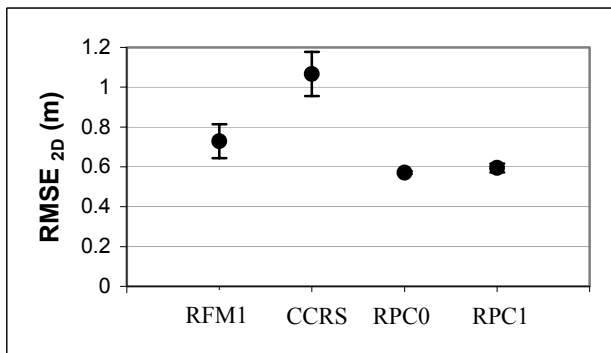


Figure 4. RMSE_{2D} over 91 ICPs with the sensor models used for 18 GCPs random sampling. The black circles represent the mean values and the error bars represent the 95% confidence interval.

The figure 4 shows the mean values and confidence intervals at 95 % of the RMSE_{2D} obtained for all 15 combinations of 18 GCPs chosen by random sampling. RFM1 and CCRS continue showing the worst results, though the values of RMSE_{2D} computed are lower enough than the presented ones in the previous figure. Now, the mean values of RMSE_{2D} are of 0.73 m for RFM1 and 1.07 m for CCRS. When RPC1 is used with 18 GCPs distributed at random, both the mean values and the standard deviations of the RMSE_{2D} diminish obviously with regard to the showed ones in the figure 3, up to close to the values obtained from RPC0. In this case, the mean values for RMSE_{2D} were 0.57 m and 0.59 for RPC0 and RPC1 respectively.

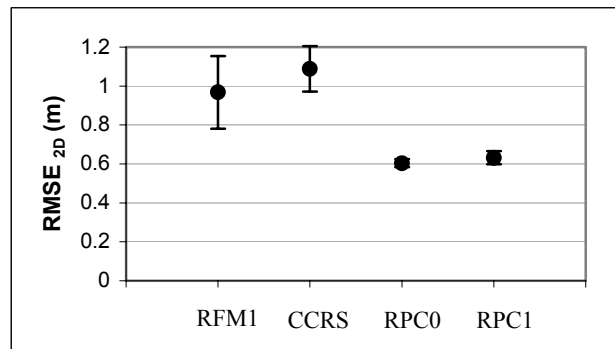


Figure 5. RMSE_{2D} over 100 ICPs with the sensor models used for 9 GCPs stratified random sampling. The black circles represent the mean values and the error bars represent the 95% confidence interval.

In the figure 5, 9 GCPs have been chosen according to a stratified random sampling. The only difference in relation to the information presented in the figure 3 is that in this occasion the 9 GCPs are well distributed along IKONOS's scene. This is due to the fact that we are taking one GCP in each one of the 9 sub-areas in which the original scene was divided. The results for all four tested sensor models are very similar to those presented in the figure 4, which were obtained from 18 GCPs with random sampling.

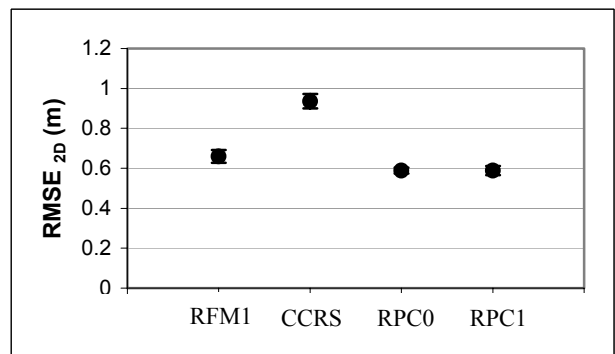


Figure 6. RMSE_{2D} over 91 ICPs with the sensor models used for 18 GCPs stratified random sampling. The black circles represent the mean values and the error bars represent the 95% confidence interval.

In the figure 6, 18 GCPs chosen according to stratified random sampling have been used. In this case, the number of GCPs is higher than the minimum necessary to calculate any of the four tested sensor models. Furthermore, they have a good distribution. The results presented for the mean values of RMSE_{2D} in RFM1 and CCRS models are slightly better than the presented ones in the figures 4 and 5, whereas the confidence intervals diminish drastically. Nevertheless, the results obtained for RPC0 and RPC1 models are very similar to those showed in the previous two figures. The standard deviations for all 15 repetitions of 18 GCPs chosen with a stratified random sampling turned out to be very small for all the tested sensor models, ranging between values of only 0.07 m for CCRS to 0.03 m for RPC0.

According to these results, it seems to be clear that the sensor model that achieved a better geometric correction of Geo Ortho Kit IKONOS image is RPC0. Besides, the results computed by RPC0 are very robust for the different numbers of tested GCPs, and does not depend on their distribution.

4.2 Orthorectified Image Error

The second test was carried out to verify the final geometric errors obtained over IKONOS orthoimages, i.e., in the final product of the orthorectification process. For it, four orthoimages were generated (one for every sensor model tested) from one of the repetitions of 18 GCPs chosen according to stratified random sampling. Four else were generated from one of the repetitions of 9 GCPs, also using stratified random sampling.

The table 2 shows the $RMSE_{2D}$ computed by comparison of the planimetric positions of all 100 points chosen in the vectorial cartography 1:1,000 of the zone (Fig. 7), against the new positions of the same points on the different orthoimages generated from IKONOS Geo Ortho kit. The mean values of $RMSE_{2D}$ obtained in the sensor orientation phase ($RMSE_O$) for all 15 repetitions of 18 GCPs from stratified random sampling, as it is showed in figure 6, are of 0.66 m, 0.94 m, 0.59 m and 0.59 m for RFM1, CCRS, RPC0 and RPC1 respectively. The $RMSE_O$ of the repetitions chosen to generate the orthoimages (table 2) is very similar to the mean values for every sensor showed above. The total $RMSE_{2D}$ measured in every orthoimage ($RMSE_{ORTHO}$) will be the sum of the errors generated in the sensor orientation phase ($RMSE_O$) and the errors due to the relief. The correction of the last one will depend on the quality of the DEM used in the orthorectification process.

The best results with regard to the IKONOS orthoimages were obtained using the rational coefficients given by the vendor (RPC0 and RPC1), reaching a $RMSE_{ORTHO}$ ranging between 1.23 m and 1.25 m. $RMSE_{ORTHO}$ produced by CCRS and RFM1 models range between 1.24 m and 1.36 m (table 2).

GCPs	Model	$RMSE_O$ (m)	$RMSE_{ORTHO}$ (m)
18	RFM1	0.67	1.35
	CCRS	0.94	1.36
	RPC0	0.58	1.25
	RPC1	0.60	1.23
9	RFM1	0.73	1.24
	CCRS	0.96	1.35
	RPC0	0.59	1.25
	RPC1	0.55	1.23

Table 2. $RMSE_{2D}$ in the different phases of the orthorectification of IKONOS's image.



Figure 7. Two points chosen on the vectorial cartography at a scale of 1:1,000 overlaid an IKONOS's orthoimage.

For flat areas, using a 5-7 m accuracy DEM and with DGPS GCPs, Wolniewicz (2004) obtained IKONOS orthoimages with a $RMSE_{ORTHO}$ of about 1.5 m. With a similar DEM ($RMSE_z < 5$ m) and GCPs, Kay *et al.* (2003) generated IKONOS orthorectified images with a $RMSE_{ORTHO}$ around 2 m. On the other hand, Davis and Wang (2003) showed $RMSE_{ORTHO}$ around 1 m measured in IKONOS orthoimages located in an urban area of Springfield, MO, using 2 m accuracy DEM. These heterogeneous results in IKONOS orthoimages are caused fundamentally for the accuracy of ancillary data (GCPs and DEM), and, with lesser importance, for the satellite view angle (Chmiel *et al.*, 2004).

5. CONCLUSION

The best results in the sensor orientation phase for IKONOS Geo Ortho Kit image were obtained when RPC0 model was used. The $RMSE_{2D}$ for sensor orientation was around 0.59 m for all studied cases computed by this mathematical approach. With RPC0, the number and distribution of the GCPs used did not influence in the results, and very small values for standard deviation (about 0.03 m) were obtained. RFM1 and CCRS models showed a great sensibility to the number and distribution of GCPs in IKONOS scene.

In matter of the orthorectified images of IKONOS, the $RMSE_{ORTHO}$ values were ranged between 1.23 m and 1.36 m. The small differences obtained with different sensor models tested in this work were owed to the very good distribution of the GCPs in the two combinations of 9 and 18 GCPs chosen for the generation of the eight orthoimages. We think that the GCPs chosen in operational conditions must have the best possible distribution, both in horizontal and in vertical, along the scene. In any case, the sensor model RPC0 generated the best results in all cases tested. Because of it, when we have the vendor's RPC file, RPC0 should be the method used in the process of orthorectification of IKONOS Geo Ortho Kit imagery.

6. ACKNOWLEDGEMENTS

The authors would like to thank the Public Enterprise for Agriculture and Fishery of Andalusia (D.a.p.) for their collaboration in the preparation of this study within the project "Basic Cartography for the Campo de Nijar (Almeria) Irrigation Project". This research work has been carried out within the project "Generation, integration and update of digital cartography as a support for rural sustainable development. Methodology and application in Campo de Nijar (Almeria)" subsidized by the Andalusia Government.

7. REFERENCES

- Aguilar, M.A., Aguilar, F.J., Sánchez, J.A., Carvajal, F. and Agüera, F., 2005a. Geometric correction of the QuickBird high resolution panchromatic images. In: *XXII International Cartographic Conference*, A Coruña, Spain. unpaginated CD ROM.
- Aguilar, F.J., Agüera, F., Aguilar, M.A. and Carvajal F., 2005b. Effects of terrain morphology, sampling density, and interpolation methods on grid DEM Accuracy. *Photogramm. Eng. Remote Sens.*, 71(7), pp. 805-816.

- Cheng, P., Toutin, T. and Zhang, Y., 2003. QuickBird-Geometric correction, data fusion, and automatic DEM extraction. In: *The 24th Asian Conference on Remote Sensing (ACRS 2003) and 2003 International Symposium on Remote Sensing*, Busan, Korea, unpaginated CD ROM.
- Cheng, P., Smith, D. and Sutton, S., 2005. Mapping of QuickBird images using the RPC method improvement in accuracy since release of first QuickBird data. *GEOInformatics*, 8(4), pp. 50-52.
- Chmiel, J., Kay, S. and Spruyt, P., 2004. Orthorectification and geometric quality assessment of very high spatial resolution satellite imagery for Common Agricultural Policy purposes. *The International Archives of the Photogrammetry, Remote Sensing and Spatial Information Sciences*, Istanbul, Turkey, Vol. XXXV, Part B4, 5 p. (On DVD).
- Davis, C.H. and Wang, X., 2003. Planimetric accuracy of Ikonos 1 m panchromatic orthoimage products and their utility for local government GIS basemap applications. *International Journal of Remote Sensing*, 24(22), pp. 4267-4288.
- Fraser, C.S., 2002. Papers of ACRS 2002 "Prospect for mapping from high-resolution satellite imagery", Kathmandu, Nepal. <http://www.gisdevelopment.net/acrs/2002/vhr/070.pdf> (accessed 5 Jun. 2005)
- Fraser, C.S., Hanley H.B. and Yamakewa, T., 2002. Three-dimensional geopositioning accuracy of Ikonos imagery. *Photogrammetric Record*, 17(99), pp. 465-479.
- Fraser, C.S., and Yamakewa T., 2004. Insights into affine model for high-resolution satellite sensor orientation. *ISPRS Journal of Photogrammetry and Remote Sensing*, 58(2004), pp. 275-288.
- Grodecki, J., and Dial, G., 2003. Block adjustment of high-resolution satellite images described by rational polynomials. *Photogramm. Eng. Remote Sens.*, 69(1), pp. 59-68.
- Jacobsen, K., 2002. Generation of orthophotos with Carterra Geo images without orientation information. In: *Proceedings of the ACSM-ASPRS Annual Conference/XXII FIG International Congress*, Washington DC, USA, unpaginated (CD ROM).
- Kay, S., Spruyt, P., Alexandrou, K., 2003. Geometric quality assessment of orthorectified VHR space image data. *Photogramm. Eng. Remote Sens.*, 69(5), pp. 484-491.
- Pecci, J., Cano, F. and Maza, G., 2004. Generación de una ortoimagen QuickBird del año 2003 de la Comunidad Autónoma de la Región de Murcia: metodología y resultados. In: *XI Congreso Métodos Cuantitativos, Sistemas de Información Geográfica y Teledetección*, Murcia, Spain. Vol. I, pp. 301-312.
- Tao, C.V. and Hu, Y., 2001. A comprehensive study of the rational function model for photogrammetric processing. *Photogramm. Eng. Remote Sens.*, 67(12), pp. 1347-1357.
- Tao, C.V., Hu, Y. and Jiang, W., 2004. Photogrammetric exploitation of IKONOS imagery for mapping applications. *International Journal of Remote Sensing*, 20(14), pp. 2833-2853.
- Toutin, T., 1995. Multi-source Data integration with an integrated and unified geometric modelling. *EARSel Journal Advances in Remote Sensing*, 4(2), pp. 118-129.
- Toutin, T., 2003. Error tracking in Ikonos geometric processing using a 3D parametric model. *Photogramm. Eng. Remote Sens.*, 69(1), pp. 43-51.
- Toutin, T., 2004. Review article: Geometric processing of remote sensing images: models, algorithms and methods. *International Journal of Remote Sensing*, 25(10), pp. 1893-1924.
- Toutin, T. and Cheng, P., 2000. Demystification of IKONOS. *Earth Observation Magazine*, 9(7), pp. 17-21.
- Toutin, T. and Cheng, P., 2002. QuickBird- A milestone for high-resolution mapping. *Earth Observation Magazine*, 11(4), pp. 14-18.
- Wong, K.W., 1980. Basics mathematics of photogrammetry. In: *manual of photogrammetry, 4th edn*, edited by C.C. Slama, American Society of Photogrammetrists, Falls Church, VA, pp. 37-101.
- Wolniewicz, W., 2004. Assessment of geometric accuracy of VHR satellite images. *The International Archives of the Photogrammetry, Remote Sensing and Spatial Information Sciences*, Istanbul, Turkey, Vol. XXXV, Part B1, 5 p. (On DVD).
- Zhou, G. and Li, R., 2000. Accuracy evaluation of ground points from IKONOS high-resolution satellite imagery. *Photogramm. Eng. Remote Sens.*, 66(9), pp.1103-1112.